Energy relaxation of lower-dimensional hot carriers studied with picosecond photoluminescence

R. W. J. Hollering,* T. T. J. M. Berendschot, H. J. A. Bluyssen,
H. A. J. M. Reinen, and P. Wyder†
*Research Institute for Materials and High Field Magnet Laboratory, University of Nijmegen, Toernooiveld,
NL-6525 ED Nijmegen, The Netherlands*

F. Roozeboom
Philips Research Laboratories, NL-5600 JA Eindhoven, The Netherlands

To study the energy relaxation of lower-dimensional hot carriers, picosecond time- and energy-resolved photoluminescence measurements have been carried out on bulk GaAs and GaAs/Al$_x$Ga$_{1-x}$As quantum-well structures in the presence of magnetic fields up to $B = 20$ T. For GaAs the results show that the energy-relaxation rate reduces with increasing strength of the magnetic field. This cooling behavior is adequately described by a model for energy relaxation containing the magnetic-field-dependent kinetics of the coupled carrier–nonequilibrium-LO-phonon system. For the quantum-well structures, an increasing magnetic field normal to the quasi-two-dimensional layers reduces the carrier cooling up to $B = 8$ T, while at higher field strengths an enhancement in cooling is observed up to $B = 20$ T. We suggest this effect to be due to a reduction in energy relaxation rate by LO-phonon emission, so that at $B > 8$ T carrier cooling is taken over by acoustic-phonon emission, which increases with magnetic field.

I. INTRODUCTION

Study of lower-dimensional carrier systems, obtained by confinement of carriers in quantum-well layers, quantum-well wires, or quantum-well boxes, is of great importance from both the fundamental and technological points of view. The ability to grow modulated semiconductor structures with dimensions in the order of the de Broglie wavelength of the carriers provides a way to modify wave functions, band structure, and scattering rates of the carriers, i.e., to modify the material parameters. Quasi-two-dimensional carrier systems exhibit interesting new physical phenomena,[1] and improved optical and transport properties which are valuable for fast (opto-) electronic devices. Quantum-well (QW) wires, in which carrier motion is quantized in two directions, and is only possible in the longitudinal direction, have been realized by Petroff et al.[2] However, to date no satisfactory QW wires have been fabricated for optical and electronic devices. Theoretical investigations on transport in QW wires predict strongly reduced scattering probabilities, which can be useful for the development of high-speed semiconductor devices. For quantum-well-box lasers, in which carrier motion is completely quantized and the carriers have a zero-dimensional character, great improvements in performance are predicted.[3]

Study of quasi-one-dimensional or quasi-zero-dimensional carrier states with dispersion relations and density of states like carriers in a QW wire and a QW box, respectively, is possible due to the confinement properties of a strong magnetic field. Determination of the energy-relaxation rate of lower-dimensional hot carriers in semiconductor materials is of fundamental importance for the understanding of the lower-dimensional carrier-phonon interactions.[4,5]

For hot quasi-two-dimensional carriers in GaAs/Al$_x$Ga$_{1-x}$As quantum-well structures, picosecond excite-and-probe, and luminescence experiments[6-12] showed a reduced relaxation rate in comparison to bulk GaAs.[13-17] As a possible origin for this reduced carrier cooling, Ryan suggested the effects of reduced dimensionality of the carrier (and phonon) system, dynamic screening by the two-dimensional (2D) plasma, and degenerate electron statistics.[7] However, recent theoretical[18] and experiment[10,19] investigations strongly indicate that nonequilibrium LO-phonon populations generated by the relaxing carriers play a predominant role in the experimentally observed reduced carrier-cooling rate.

In this paper we describe in detail the results of a study on hot-carrier energy relaxation in the presence of a strong magnetic field (up to $B = 20$ T) for both bulk GaAs and GaAs/Al$_x$Ga$_{1-x}$As quantum-well structures by time and energy-resolved picosecond photoluminescence. Analysis of the time- and energy-resolved photoluminescence spectra with a model containing the density of states for electrons and holes and the Fermi distribution functions yields the temperature $T_{e,h}(t)$ and density $n_{e,h}(t)$ of the carriers, and for $B \neq 0$ T the Landau-level linewidth $\Gamma(t)$ as a function of time after excitation.

From this analysis it was found that under picosecond photoexcitation the energy-relaxation rate for hot carriers in bulk GaAs and GaAs/Al$_x$Ga$_{1-x}$As quantum-well structures is strongly affected by a magnetic field. For GaAs the results show that the energy-relaxation rate reduces with increasing strength of the magnetic field and that the carrier cooling is adequately described

by a model for energy relaxation containing the magnetic-field-dependent kinetics of the coupled carrier-nonequilibrium optical-phonon system. The observed magnetic-field dependence of the carrier cooling and the absence of magnetophonon resonances support the assumption of the presence of nonequilibrium optical-phonon distributions generated by the relaxing carriers.

For the quantum-well structures application of a magnetic field parallel to the GaAs layers clearly shows the two-dimensional character of the carrier gas, and the energy-relaxation rate was found to be independent of field strength as long as the cyclotron orbit diameter exceeds the quantum-well width. For a field direction normal to the layers an increase in magnetic-field strength reduces the relaxation rate via optical-phonon emission, as in three dimensions. At high magnetic fields $(B > 8$ T) an enhanced cooling was observed, which we suggest to be due to an increasing relaxation via acoustic-phonon emission.

This paper is organized as follows. Section II describes the sample properties and experimental procedures for picosecond-time- and energy-resolved photoluminescence measurements under application of strong magnetic fields. Also, experimental results of the time-resolved luminescence experiments on bulk GaAs and GaAs/Al$_x$Ga$_{1-x}$As quantum wells, respectively, are presented. In Sec. III the procedure to analyze the luminescence spectra is presented, and as a first result the time variation of the Landau-level-broadening parameter $\Gamma(t)$, which describes the evolution of the initially strongly broadened Landau-level density of states, is discussed. In Sec. IV a theory for hot-carrier energy relaxation in the presence of a magnetic field is briefly discussed. For bulk GaAs a model was used that contains the magnetic-field-dependent coupled carrier-phonon interaction rates, and takes into account the nonequilibrium optical-phonon populations generated by the relaxing carriers. To describe the increasing energy relaxation with magnetic-field strength for hot quasi-2D carriers at $B > 8$ T the results of a model calculation on the relaxation via acoustic-phonon emission are presented. Section IV B gives the experimental results on the carrier cooling and a comparison with theory is made. Finally in Sec. V the results obtained from the analysis and the physics underlying the observed variations in energy relaxation are discussed.

II. EXPERIMENTAL DATA AND RESULTS

The photoluminescence experients were carried out on unintentionally doped bulk GaAs and GaAs/Al$_x$Ga$_{1-x}$As quantum-well structures, grown by metal organic vapor-phase epitaxy (MOVPE) in a specially designed reactor cell, the details of which are given elsewhere.[20] The background doping level in bulk GaAs was determined from Hall measurements to be 1×10^{15} cm^{-3} and is expected to be the same for the quantum-well structures. The bulk GaAs sample was grown on an n-type GaAs substrate, and consists of a 0.25-μm-thick GaAs layer, confined between 0.1-μm-thick Al$_{0.6}$Ga$_{0.4}$As barrier layers. These confining layers are transparent to the excitation wavelength and avoid surface recombination and carrier diffusion to the substrate and reduce the gradient in carrier density perpendicular to the surface. The quantum-well structures were grown on GaAs buffer layer on the substrate, and consist of five periods of 5-nm GaAs and 100-nm Al$_{0.6}$Ga$_{0.4}$As. The various layer thicknesses were determined by means of transmission electron microscopy (TEM).

Optical excitation was achieved with picosecond light pulses (duration 2 ps) from a cw dye laser (rhodamine-6G dye, emission wavelength 610 nm), which is synchronously pumped by a mode-locked Kr-ion laser (repetition rate 82 MHz). Time-resolved detection of the emitted luminescence radiation due to electron-hole recombination, was performed with use of an up-conversion light-gating technique.[12,21,22] The picosecond laser pulses are split into two pulse trains, of which one focused by a microscope objective to a 15-μm-diam spot on the sample surface, while the other is sent through a stepping-motor-controlled variable-delay path. The luminescence from the epilayers is collected by the same objective, and focused collinearly with the delayed picosecond light pulse onto a LiIO$_3$ crystal. The 3-mm-thick crystal, cut with the optic axis at 58° to the surface normal, is angle tuned with a stepping motor, to generate sum-frequency radiation. The phase-matching bandwidth for up-conversion in the LiIO$_3$ crystal, is experimentally determined to be 12 nm [full width at half maximum (FWHM)]. Due to group-velocity mismatch of the luminescence radiation and the picosecond light pulses the time resolution of the light-gate system is 5 ps. The up-converted signal is detected with an EMI 9789/82 QB photomultiplier tube via a 1-m grating monochromator (Monospek) with 0.5-nm spectral resolution. To measure the spectral distribution of the luminescence radiation at a fixed delay time, the phase-matching angle of the nonlinear optical crystal is synchronously tuned with the monochromator. The spectral response of the complete photodetection system was calibrated with use of a quartz halogen lamp and taken into account in the analysis of the measurements. To allow lock-in detection techniques the excitation beam is mechanically chopped.

The samples were cooled down to a temperature of 1.5 K in a bath cryostat, which was mounted in the hybrid magnet system of the University of Nijmegen. This magnet, which delivers fields up to 25 T dc, consists of a two-segment Bitter coil surrounded by an 8-T superconducting magnet.

To study the energy relaxation of hot carriers generated with a picosecond laser pulse in GaAs the excitation beam with an average excitation power of 2.7 mW (photon flux per pulse 5×10^{13} cm^{-2}) was focused onto the sample surface. Estimation of the initially excited electron-hole density by taking into account a reflection coefficient of $R = 0.3$ and an absorption coefficient of $\alpha = 4 \times 10^4$ cm^{-1} amounts to $n_{e,h}(t=0) = 1 \times 10^{18}$ cm^{-3}.

Figure 1 shows the measured and calculated (see Sec. III) luminescence spectra due to electron-hole recombination at different delay times up to 850 ps after excitation in the absence of a magnetic field. Under the experimental conditions (i.e., high-excitation intensity, high-quality
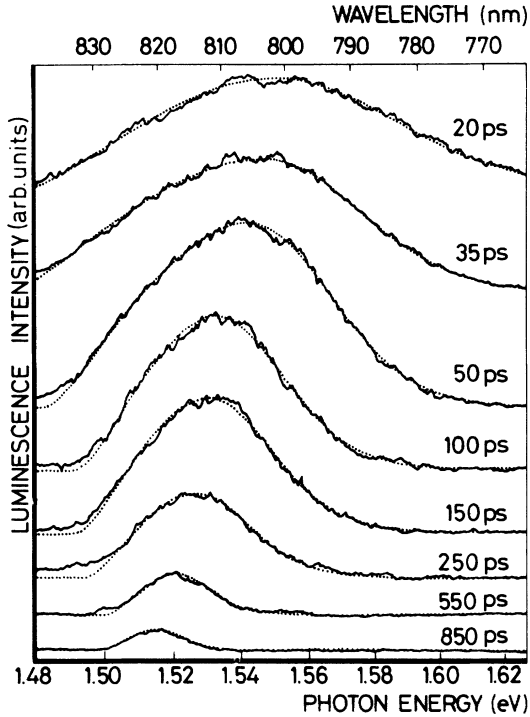
FIG. 1. Measured and calculated (dots) photoluminescence spectra of bulk GaAs at different delay times after excitation. The spectra are all drawn on the same vertical scale to show the real-time evolution for the different photon energies. Values for density $n_{e,h}(t)$ and temperature $T_{e,h}(t)$ of the carriers were obtained from an analysis of these spectra.
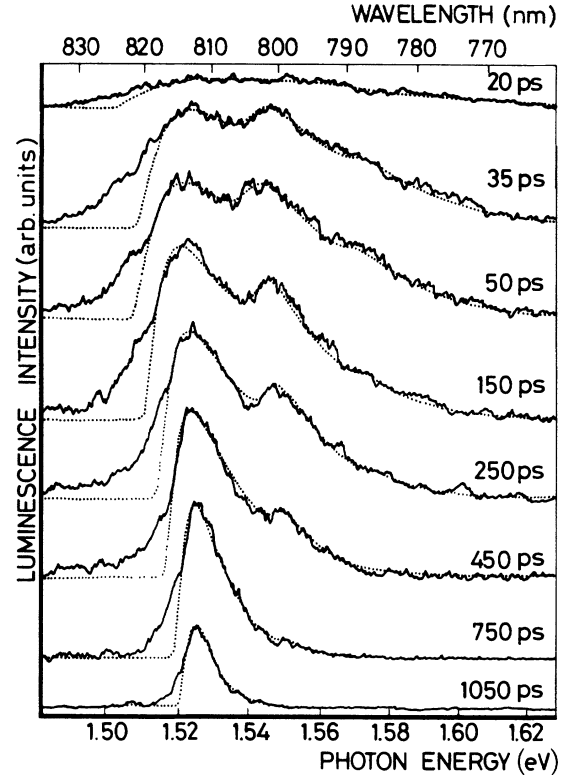

FIG. 2. Measured and calculated (dots) time- and energy-resolved luminescence spectra of bulk GaAs in the presence of a magnetic field of $B = 16$ T. Value for density $n_{e,h}(t)$ and temperature $T_{e,h}(t)$ of the carriers and Landau-level linewidth $\Gamma(t)$ were obtained from analysis of these spectra.

GaAs) luminescence radiation emitted by the epilayer is due to free carrier recombination and thus contains information about the energetic distributions of the carriers in the bands.[23] The spectra are all drawn here on the same vertical scale to depict the time evolution of the luminescence signal for the different photon energies. With respect to the low-energy side of the luminescence spectra, a shift to higher photon energies with increasing delay time is observed, which is related to a decrease in the carrier density, and therefore a shift of the renormalized band gap.[15] Obviously the change in slope on the high-energy side of the spectra is directly related to the decreasing carrier temperature with time (see Sec. III).

Similar spectra, but in the presence of a magnetic field of 16 T, are presented in Fig. 2 and show Landau-level structure arising at 35 ps after excitation, when both the thermal energy of the carriers, $k_B T_{e,h}$, and the Landau-level linewidth Γ are less than the Landau-level splitting $\hbar\omega_c$. Due to both cooling (relaxation) and recombination of electrons and holes, occupation of higher Landau levels decreases, which is clearly shown by the decreasing spectral range of the luminescence spectra. This results finally in population of only the $N = 0$ Landau level at times exceeding 750 ps after excitation.

We now turn to the experimental results on the energy relaxation of hot carriers confined in quantum-well structures. In the sample used, of which the parameters are given above, the band gap of the $Al_{0.6}Ga_{0.4}As$ confining

layers exceeds the laser photon energy, and excitation with an average power of 2.4 mW created an initial carrier density of 3×10^{18} cm^{-3} directly in the thin GaAs layers. Restricting the number of GaAs wells to five minimizes reabsorption of luminescence radiation and ensures a homogeneously excited carrier density in the different layers (variation less than 5%). In Fig. 3 some time-resolved 2D subband luminescence spectra are shown for $B = 0$ T (thin lines) and $B = 8$ T normal to the layers. In both cases the spectra distributions consist of a broad luminescence band with features comparable to the corresponding 3D spectra.[23] Direct comparison of the slopes at the high-energy side of the corresponding $B = 0$ and 8 T spectra reveals the much higher carrier temperatures for the latter except at 25 ps. Due to well-width fluctuations, which give rise to varying Landau-level energies, the luminescence spectra are broadened and no Landau-level structure is observed at $B = 8$ T. This phenomenon will be discussed in Sec. III (see Fig. 7).

By increasing the magnetic field up to 20 T, Landau-level structure is clearly observed in the spectra of Fig. 4 at times from 75 ps after excitation. With increasing delay time the carriers cool down by photon emission and recombine, which both lead to a depopulation of the higher Landau levels, as shown by the decreasing spectral range of the subsequent spectra. It should be noticed that comparison of the symmetric spectra line shapes of the quantum-well luminescence spectra (Fig. 4) with the
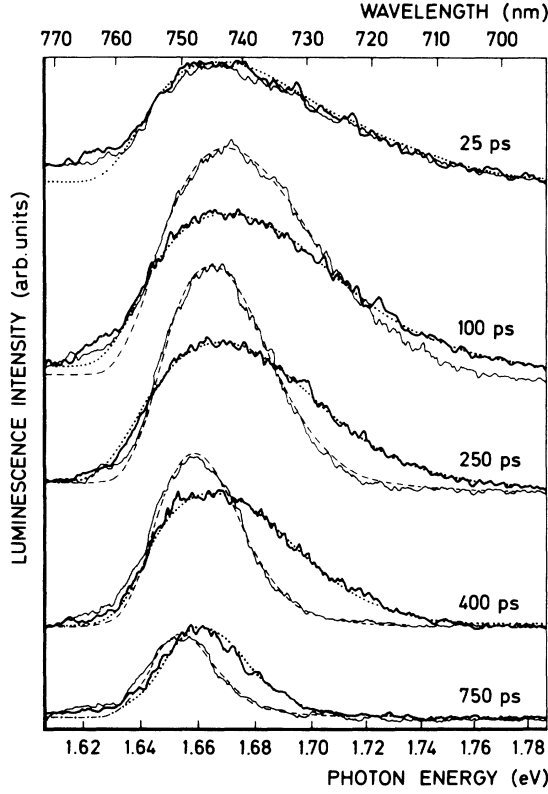
FIG. 3. Measured and calculated subband luminescence spectra of a GaAs/As$_{0.6}$Ga$_{0.4}$As quantum-well structure at different times after excitation for $B = 0$ T (thin lines) and $B = 8$ T normal to the layers. Comparing the slopes of the spectral high-energy tails of the corresponding spectra shows that carrier cooling at $B = 8$ T is reduced with respect to $B = 0$ T.
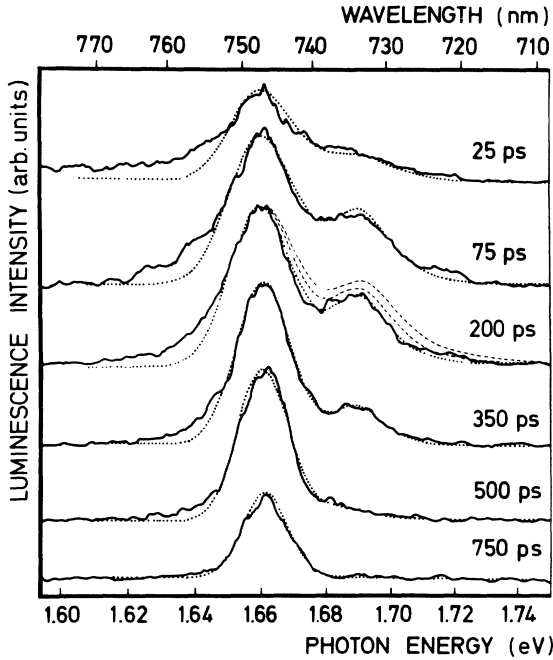

FIG. 4. Measured and calculated time- and energy-resolved luminescence spectra of a GaAs/Al$_{0.6}$Ga$_{0.4}$As quantum-well structure for $B = 20$ T normal to the layers. The dashed lines at 200 ps are due to a variation of 10 K in carrier temperature, and show the sensitivity of the fitting procedure.

asymmetric line shapes for the bulk GaAs spectra (Fig. 2) reflects the different Landau-level density of states for the quasi-2D and -3D carrier gases, respectively (see Sec. III).

III. ANALYSIS

Direct one-photon interband absorption of a picosecond light pulse creates instantaneously monoenergetic electron and hole distributions in conduction and valence bands, which thermalize by carrier-carrier interactions within a picosecond to an effective temperature $T_{e,h}$ far above the lattice temperature.[17] In order to obtain temperature $T_{e,h}(t)$ and density $n_{e,h}(t)$ of the carriers, and for $B \neq 0$ the Landau-level linewidth $\Gamma(t)$ at different delay times t after excitation, the measured photoluminescence spectra (Figs. 1–4) due to electron-hole (band-to-band) recombination were analyzed with a model neglecting the k-selection rule[15] as is given by

$$I(\hbar\omega) = C \int_0^{\hbar\omega - E_1} g_c(E)g_v(\hbar\omega - E - E_1)f_c(E)$$

$$\times f_v(\hbar\omega - E - E_1)dE , \qquad (1)$$

where C is a constant which contains the optical matrix element. For bulk GaAs, E_1 represents the renormalized energy gap[15] formed by conduction and valence bands ($E_1 = E_g$), while for the quasi-two-dimensional case $E_1 = E_g + E_{1e} + E_{1h}$ where E_{1e} and E_{1h} are the lowest 2D quantum-well subbands. It should be noticed that, due to one-well-width fluctuation δL_z over the spot size of the excitation beam, there is a fluctuation in E_1 given by $\delta E_{1e,1h} \approx (2E_{1e,1h})\delta L_z$.[24] These fluctuations, which influence the low-energy side of the quantum-well luminescence spectra, can be described by assuming Gaussian distributions of E_1.[25] This is accomplished by inserting in front of Eq. (1) the integral

$$(2\pi\Gamma'^2)^{-1/2} \int \exp[-(E_1 - \langle E_1 \rangle)^2/2\Gamma'^2]dE_1$$

where $\langle E_1 \rangle$ is the expectation value of E_1 and Γ' can be determined from the luminescence spectra at very low excitation intensity. The Fermi-distribution functions $f_{c,v}(E)$ for electrons and holes contain the quasi-Fermi-levels $F_{e,h}$ which were determined from the relation $n_{e,h} = \int g_{c,v}(E)f_{c,v}(E)dE$. Both temperature $T_{e,h}(t)$ and density $n_{e,h}(t)$ were assumed to be similar for electrons and holes.[15,17] The density-of-states functions for the conduction (c) and valence (v) bands of a 3D gas in the presence of a magnetic field are due to Dingle, given by[26]

$$g_{c,v}^{3D}(E) = \frac{1}{2\pi l^2}\left[\frac{m^*}{\pi\hbar^2}\right]^{1/2}$$

$$\times \sum_{N=0}^{\infty}\left[\frac{(E - E_N) + [(E - E_N)^2 + \Gamma^2]^{1/2}}{(E - E_N)^2 + \Gamma^2}\right]^{1/2} , \qquad (2)$$

where $l = (\hbar/eB)^{1/2}$ is the magnetic length, m^* the carrier effective mass, $E_N = (N + \frac{1}{2})\hbar\omega_c$, with N the Landau-level index and ω_c the cyclotron frequency. For the carrier masses the values of $m_e = 0.068m_0$ and

$m_h = 0.5m_0$ have been used. Following Dingle[26] the Landau levels have a Lorentzian linewidth $\Gamma = \hbar/2\tau$,[27] where $1/\tau$ represents the carrier-scattering rate.

The experimentally observed Landau-level structure could be analyzed correctly only if the $N = 0$ term in Eq. (2) is replaced by a term calculated from Kubo's theory.[28,29] The resulting "adjusted" density-of-states function together with the result obtained from Eq. (2) are shown for electrons in Fig. 5 for $B = 20$ T. Instead of the low-energy tail into the energy gap given by Dingle's expression, a low-energy cutoff shifts to higher energies with increasing magnetic field and ensures the approach to the zero-field density of states for large Landau-level linewidths.

Further nonparabolicity of the GaAs conduction band[30] and a $\Delta N = 0$ selection rule were taken into account. Contribution of light-hole and split-off-hole valence bands may be neglected.[31] Reabsorption effects, which lower the apparent temperature slightly, were not taken into account since they are expected to work out identically for $B = 0$ T and $B \neq 0$ T and to be of minor importance. Also, spin splitting (0.026 meV/T) is neglected, since it is small compared to $k_B T_{e,h}$ and to the Landau-level splitting for electrons (1.7 meV/T) and holes (0.24 meV/T).

For the quantum-well structures the density-of-states function in the presence of a magnetic field normal to the 2D gas is given by a summation over (Gaussian) broadened Landau levels, with degeneracy $1/2\pi l^2$ as[32]

$$g_{c,v}^{2D}(E) = \frac{1}{2\pi l^2} \left[\frac{\pi}{2} \Gamma^2 \right]^{-1/2} \sum_{N=0}^{x} \exp \left[-2 \left[\frac{E - E_N}{\Gamma} \right]^2 \right].$$

(3)

For the electrons, nonparabolicity of the conduction band is taken into account. The masses of heavy and light holes are anisotropic and values for motion normal to the layers [$m_{HH}^{\perp} = 0.45m_0$ and $m_{LH}^{\perp} = 0.094m_0$ (Ref. 33)] used to calculate subband energies strongly differ from the in-plane hole masses. For motion parallel to the layers (which is relevant in our experiment) dispersion is very complicated.[3] However, Yang and Sham have analyzed magnetooptical spectra comparing parabolic bands and more realistic band structures for the valence band.[35] Their results show that the assumption of a parabolic band (with $m_{HH} = m_0$) gives a good description to within 5%. Therefore Eq. (3) is also used to describe the valence-band density of states. Moreover, to minimize the effect of band-structure complexities, very thin quantum wells ($L_z = 5$ nm) were used, where only one electronic subband is present and the energy splitting between light-hole (LH) and heavy-hole (HH) bands is 42 meV. Finally, it must be emphasized that the electron population dominates the structure of the luminescence spectrum and that the obtained carrier temperature, which follows from the high-energy side of the luminescence spectrum, is mainly governed by the electron Fermi function. Excitonic effects have not been taken into account, since the density of excited carriers is high ($n_{e,h} \approx 3 \times 10^{18}$ cm^{-3}) and variation of the Sommerfeld factor over the spectral range is less than 10%. Finally, it should be mentioned that Haug and Tran Thoai[36] have shown that carrier temperature and density obtained from a non-k-selection-rule fit are in good agreement with data obtained from exact calculations.

The calculated lines in Figs. 1–4 give a good fit at the high-energy side of the spectra, which implies that the carriers are thermalized. On the other hand, accurate analysis of the low-energy side of the spectra is very complicated, since in addition to band-gap renormalization, plasma screening of the exciton enhancement of the matrix element, plasmon effects, and tail states have to be considered.[9,22] These effects play a minor role at the high-energy tail of the luminescence spectra, which is dominated by the carrier temperature. For the spectrum at 500 ps of Fig. 4, where only the lowest Landau level is populated, the carrier density obtained by the fitting procedure is 1.8×10^{18} cm^{-3}.[12] Comparison to the maximum number of carriers per Landau level at this field value $1/\pi^2 = 2 \times 10^{18}$ cm^{-3} (where a factor of 2 for both spin states is included), shows excellent agreement. In conclusion, we have shown that the above-used analysis gives good results for both 3D and quasi-2D carrier systems ($L_z = 5$ nm) in the presence and absence of magnetic fields.

As a first result of the analysis, we concentrate on the Landay-level linewidth $\Gamma(t)$ as a function of time for bulk GaAs at $B = 16$ T as shown in Fig. 6 and derived from
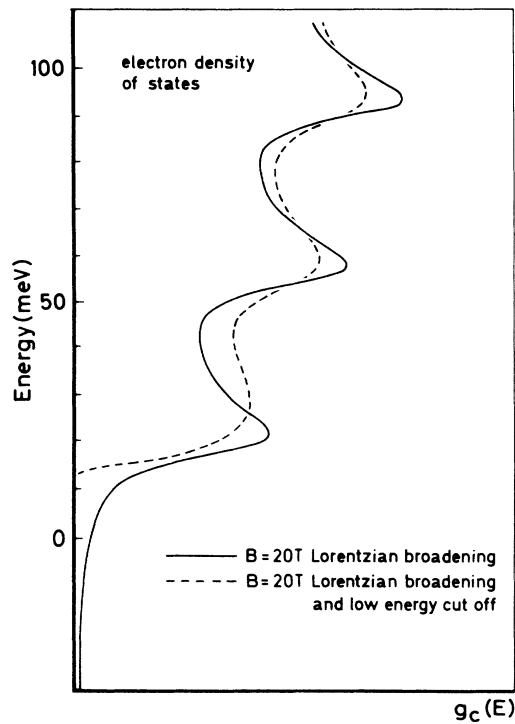

FIG. 5. Landau-level density-of-states functions calculated from Dingle's expression [Eq. (2)] and the "adjusted" expression (see text), respectively, for $B = 20$ T. The low-energy tail of the former is replaced by a low-energy cutoff of the latter. This ensures a correct shift to higher energies with increasing field strength, and the approach to the zero-field density of states for large Landau-level linewidths.
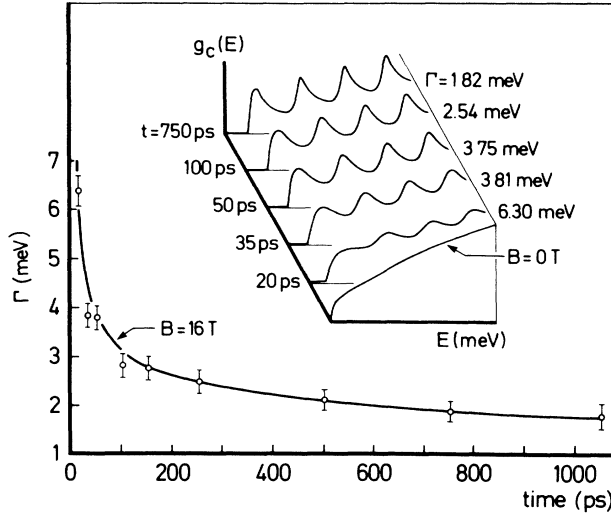
FIG. 6. Landau-level linewidth $\Gamma(t)$ for bulk GaAs as a function of time t after excitation for $B = 16$ T. The inset shows the evolution of the broadened Landau-level density of states, as determined from the spectra of Fig. 2.

the spectra of Fig. 2. The level broadening Γ (Refs. 26–29) is due to the finite lifetime of a carrier state, which for carrier temperatures $T_{e,h} \geq 50$ K mainly arises from the interaction with optical phonons. The absolute value of Γ of several meV corresponds to an expected scattering time of a few tenths of a picosecond, while the time dependence is in agreement with a reduction of the carrier density and the nonequilibrium phonon population. The inset of Fig. 6 shows the evolution of the electronic density-of-states function as derived from the spectra of Fig. 2.

For the quantum-well structures the observed broadening of the Landau-level luminescence Γ, as shown in Fig. 7, is due to a time-dependent Landau-level broadening
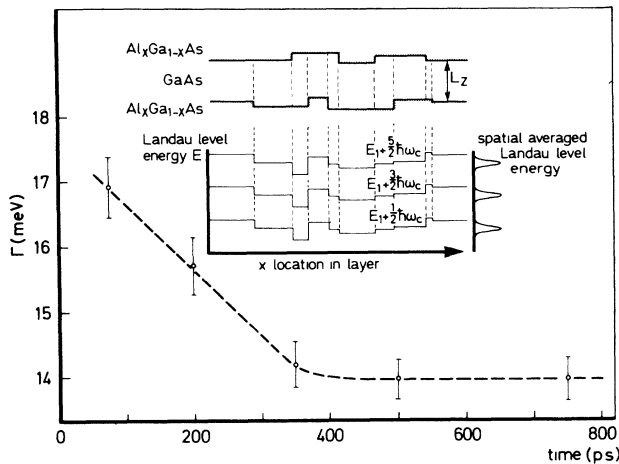

FIG. 7. Evolution of the Landau-level linewidth $\Gamma(t)$ in a GaAs/Al$_{0.6}$Ga$_{0.4}$As quantum-well structure for $B = 20$ T, as obtained by fitting the spectra of Fig. 4. The line is drawn as a guide to the eye. The inset shows the contribution to the Landau-level broadening as a result of spatial averaging over the varying Landau-level energies caused by well-width fluctuations.

Γ_{sc} and a broadening due to well-width fluctuations $\Gamma_{\delta L_z}$. Γ_{sc} depends on temperature and density of the carriers, phonon occupation number, and magnetic-field strength. This contribution is a few meV as in bulk GaAs. In addition to the broadening of the individual Landau levels, the luminescence spectra are broadened due to well-width fluctuations δL_z. The inset of Fig. 7 shows the varying Landau-level energies for the different positions in the quantum well caused by well-width fluctuations. Spatial averaging over the laser focus spot gives rise to inhomogeneous Landau-level broadening $\Gamma_{\delta L_z}$. For the quantum-well width of 5 nm, low-excitation photoluminescence measurements with a He-Ne laser yielded a value of $\Gamma_{\delta L_z} = 14$ meV, which corresponds to[24] $\delta L_z = 0.28$ nm. The total broadening Γ, as determined experimentally, is given by $\Gamma = (\Gamma_{sc}^2 + \Gamma_{\delta L_z}^2)^{1/2}$, where Γ_{sc} ranges from 10 meV at 25 ps after excitation to 1.5 meV at 500 ps after excitation for $B = 20$ T ($\hbar\omega_c = 34$ meV) comparable to bulk GaAs values. It should be noted that the overlap between the Landau levels as observed in Fig. 4 is mainly due to the inhomogeneous part of the Landau-level linewidth $\Gamma_{\delta L_z} = 14$ meV. However, for the analysis of the time evolution of the carrier temperature only the homogeneous part of the Landau-level linewidth Γ_{sc}, which is due to phonon interaction, has to be taken into account. Since in most of the cases the Landau-level splitting $\hbar\omega_c > \Gamma_{sc}$, optical-phonon emission is reduced and acoustic-phonon emission has to be brought in.

Other results from the above-described analysis are temperature $T_{e,h}(t)$ and density $n_{e,h}(t)$ of the carriers as a function of time t. The time evolution of the carrier temperature after excitation is shown in Figs. 8 and 9 for
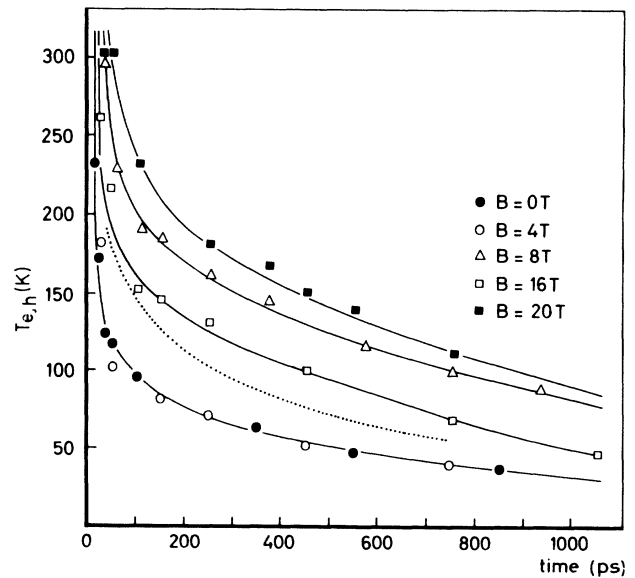

FIG. 8. The solid lines show calculated cooling curves for bulk GaAs with a model containing the (magnetic-field-dependent) kinetics of the coupled carrier-phonon system for $B = 0$, 4, 8, 16, and 20 T at $n_{e,h} = 1 \times 10^{18}$, 1×10^{18}, 3×10^{18}, 1×10^{18}, and 1×10^{18} cm^{-3}, and $C = 0.5$, 0.5, 0,5, 0.2, and 0.2. The dashed line represents the corrected cooling curve for $B = 8$ T, $n_{e,h} = 1 \times 10^{18}$ cm^{-3}, and $C = 0.5$.

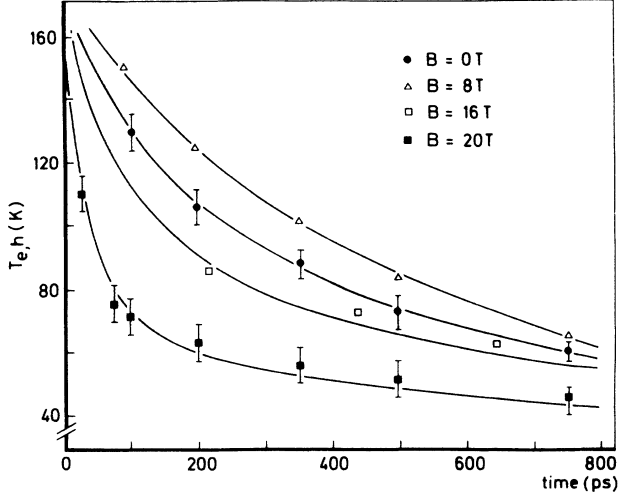FIG. 9. Carrier temperature $T_{e,h}(t)$ as a function of time t for a GaAs/Al$_{0.6}$Ga$_{0.5}$As quantum-well structure at $B=0$, 8, 16, and 20 T. The solid lines are not calculated but serve as a guide to the eye.

bulk GaAs and a 5-nm GaAs/Al$_{0.6}$Ga$_{0.4}$As quantum well, respectively.

Figure 8 shows that, in the absence of a magnetic field, carrier cooling by optical-phonon emission (see Sec. IV), which is dominant for $T_{e,h} > 50$ K,[15] practically completed within 100 ps, in agreement with previous reports.[13–16] The results show further that application of a magnetic field reduces carrier cooling in bulk GaAs substantially up to the maximum field used, of $B = 20$ T.

As to the GaAs quantum well, the results of Fig. 9 show in the first place that the carrier-cooling rate at $B = 0$ T is strongly reduced with respect to that in bulk GaAs. This is in agreement with results of other groups.[7–12] Secondly, it follows that the effect of a magnetic field strongly deviates from that in bulk GaAs. While initially the cooling rate is reduced up to about $B = 8$ T, it starts thereafter to increase up to the maximum field value of $B = 20$ T.

In the next section we will show that the experimentally determined magnetic-field dependence of $T_{e,h}(t)$ can be described by a model for hot-carrier energy relaxation that takes into account (1) for bulk GaAs both the magnetic-field-dependent carrier-phonon interaction with inclusion of nonequilibrium optical phonons and degenerate carrier statistics, and (2) for a GaAs quantum well the magnetic-field dependence of acoustic-phonon emission.

IV. HOT-CARRIER ENERGY RELAXATION

A. In bulk GaAs

At carrier temperatures $T_{e,h} > 50$ K, the excess energy of the photoexcited carrier gas is transferred to the lattice mainly by emission of optical phonons via electron– and hole–LO-phonon coupling.[17,37] The holes also interact with the TO phonons via optical deformation-potential coupling. At lower carrier temperatures the energy re-

laxation is much slower, and is mainly due to acoustic-(ac) phonon emission.

In general, the energy-relaxation rate by optical- and acoustic-phonon emission is given as[18]

$$\frac{dE}{dt} = -\sum_i \sum_q \hbar\omega_q \left[\frac{dN_q}{dt}\right]_i , \tag{4}$$

where summations run over the different carrier-phonon couplings ($i =$ LO, TO, ac) and over the wave vectors q of the phonons with energy $\hbar\omega_q$ which are involved in the energy-relaxation profess. The term $(dN_q/dt)_i$ represents the change in phonon population due to electron- (hole-) phonon interaction, and depends on temperature $T_{e,h}$ and density $n_{e,h}$ of the carriers and on the phonon occupation number N_q. The rate of change in N_q is determined from the sum of phonon generation and decay rates as

$$\left[\frac{dN_q}{dt}\right] = \left[\frac{dN_q}{dt}\right]_i - \frac{N_q - N(T_1)}{\tau} . \tag{5}$$

Here the second term on the right-hand side represents the decay rate of the generated nonequilibrium population of optical phonons into acoustic phonons, where τ is a wave-vector-independent phonon lifetime,[18] T_1 is the lattice temperature, and N is the Bose-Einstein distribution function. Following this approach, Pötz and Kocevar calculated the carrier cooling in the absence of a magnetic field.[18]

We extended their model by calculating[38] the energy-relaxation rate in the presence of a magnetic field using a field-dependent $(dN_q/dt)_i$ for unbroadened Landau levels as given by Bauer et al.[39] The application of a magnetic field changes the band structure (Landau levels) and, as a result of energy and momentum conservation, the range of involved phonon wave vectors (volume of the phonon momentum space) and the rate $(dN_q/dt)_i$. To compare the experimentally obtained temperature evolutions $T_{e,t}(t)$ with the calculated energy-relaxation rates, the relation $dE/dt = (dT_{e,h}/dt)(dE/dT_{e,h})$ was used, and we solved the coupled differential equation for $T_{e,h}$ and N_q. Here $(dE/dT_{e,h})$ is the specific heat of the carrier gas, which is taken to be $1.5k_B$ in the whole magnetic-field range. Finally, to fit the experimental data of Fig. 8 with the calculated time evolution of $T_{e,h}$, the initial temperature T_0, and a constant C (multiplication factor in front of dE/dt) have been used as adjustable parameters.

The solid lines in Fig. 8 represent the calculated cooling curves for $T_0 = 800$ K, where the values of C are given in the caption and discussed in Sec. V. For all field values the carrier cooling is adequately described by the above-presented model, the details of which are given elsewhere.[38]

It should be noticed that comparison of the carrier-cooling rates at different field strengths is only allowed

for equal carrier densities. The density of the carrier gas, which was also obtained from the spectral analysis,[15] varies from 9×10^{17} cm^{-3} directly after excitation to 1×10^{17} cm^{-3} at 1 ns (Ref. 38) and is practically similar for $B = 0$, 4, 16, and 20 T. However, due to a variation in excitation density at $B = 8$ T the carrier density is a factor of 3 higher during the entire time interval. Correction for this higher density[38] with use of the model presented above yields the dashed cooling curve for $B = 8$ T, which fits extremely well in the magnetic-field dependence of the other experimentally determined cooling curves.

In conclusion, it is shown that (1) the model which takes into account both a nonequilibrium optical-phonon distribution and degenerate carrier statistics gives a good description of the experimental data, and (2) for a 3D carrier gas the energy-relaxation rate reduces with increasing magnetic field up to $B = 20$ T.

B. In quantum-well structures

Comparison of the experimentally determined cooling curves of Figs. 8 and 9 shows that the carrier-cooling rate at $B = 0$ T in the 5-nm GaAs quantum wells is strongly reduced with respect to bulk GaAs.

From the slope of the zero-field-cooling curve it follows that for 2D carriers the experimentally determined energy-relaxation rate is of the order of -1×10^7 eV/s. This implies that the contribution of acoustic phonons to the energy relaxation cannot be neglected,[40] as is usually done for $T_{e,h} > 50$ K.[6-10]

To get some insight in the magnetic-field dependence of the energy relaxation via acoustic-phonon emission $(dE/dt)_{ac}$, a model calculation was performed using a general expression for phonon emission and absorption as given by Conwell.[41] The influence of the magnetic field on scattering in the plane of the layers enters the model via the transition matrix element between the different Landau levels. The effect of confinement on the carrier-phonon coupling in the quasi-2D layers is treated using the analytical approach of Price.[42] Fermi-Dirac statistics was used to describe the carrier system, while the phonon system was assumed to behave three dimensionally. The Landau levels were taken to be Gaussian broadened. Complexities concerning the valence-band structure, which may influence the energy-relaxation rate, were not taken into account, and parabolic bands were assumed. The calculations, of which more details are given elsewhere,[43] show that $(dE/dT)_{ac}$ is a function of magnetic-field strength B, Landau-level linewidth Γ, carrier-density $n_{e,h}$, and carrier-temperature $T_{e,h}$. In our temperature region the Landau-level broadening Γ is caused mainly by electron-phonon interaction.[44] A measure for this interaction with the optical and acoustic phonons is the energy-relaxation rate (dE/dt) itself. There Γ should be calculated self-consistently.[32] However, Γ can be determined experimentally, which enables us to insert the measured value for Γ into the calculations. In this way in our analysis the influence of the Landau-level broadening on the energy relaxation is taken into account automatically.[43] Results of these model calculations show
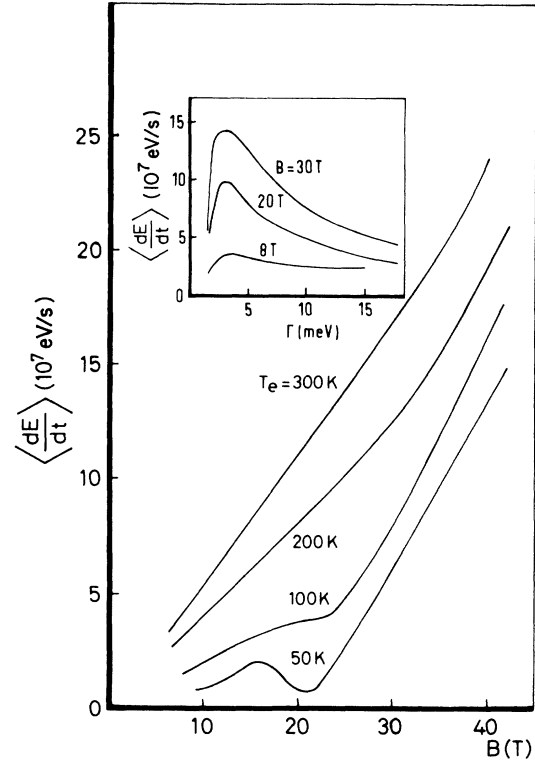

FIG. 10. Energy-relaxation rate by acoustic-phonon emission as a function of magnetic field for fixed carrier temperature $T_{e,h}$. The inset gives the value of $(dE/dt)_{ac}$ as a function of Landau-level linewidth Γ for fixed field strengths at $T_{e,h} = 150$ K.

that (1) $(dE/dt)_{ac}$ is of the order of 10^7 eV/s and has to be taken into account, and (2) the importance of relaxation via acoustic-phonon emission increases with field strength.

Figure 10 shows the increasing energy-relaxation rate for quasi-2D carriers by acoustic-phonon emission as a function of magnetic field for different carrier temperatures at a carrier density $n_{e,h} = 2 \times 10^{18}$ cm^{-3} and a Laudau-level linewidth of 7 meV. The oscillations in the value of $(dE/dt)_{ac}$ at $T_{e,h} = 50$ K and $T_{e,h} = 100$ K as a function of field strength, are related to the position of the Fermi level with respect to the Landau levels. The origin of the oscillations is similar to that of the de Haas–van Alphen effect. The inset of Fig. 10 gives the value of $(dE/dt)_{ac}$ as a function of Γ for fixed field strengths at $T_{e,h} = 150$ K and $n_{e,h} = 2 \times 10^{18}$ cm^{-3}. If $\Gamma = 0$, i.e., the density of states consists of δ functions, no intra-Landau-level emission of phonons is allowed, thus $(dE/dt)_{ac}$ is zero. On the other hand, for very large value of Γ the energy loss becomes small again because the peak of the Landau levels is proportional to $1/\Gamma$. Therefore $(dE/dt)_{ac}$ has a maximum for $\Gamma = 3$ meV which corresponds to the energy of the acoustic-phonon mode with the largest wave vector that can participate in the scattering, determined by the matrix elements. For small magnetic-field strengths the maximum is less pronounced due to the increasing Landau-level overlap. The
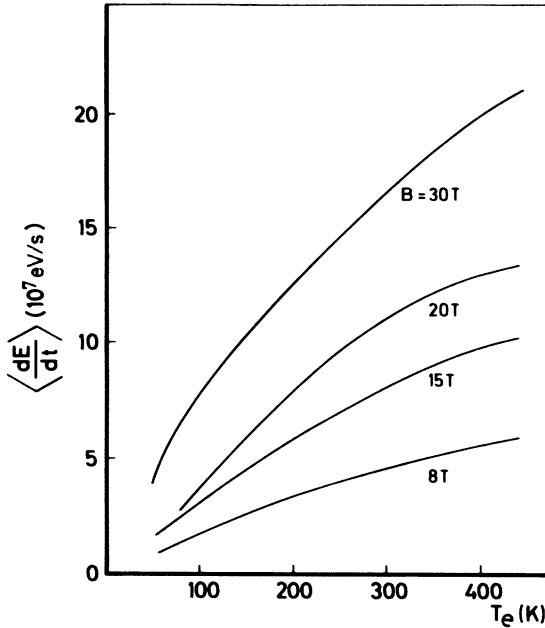
FIG. 11. The calculated energy-relaxation rate due to acoustic-phonon scattering as a function of carrier temperature for $B = 8$, 15, 20, and 30 T, $\Gamma = 7$ meV, and $n_{e,h} = 2 \times 10^{18}$ cm^{-3}.

FIG. 12. Time to cool down to $T_{e,h} = 100$ K as a function of magnetic-field strength for hot carriers in GaAs (solid line) or in a 5-nm GaAs/Al$_{0.4}$Ga$_{0.6}$ As quantum-well structure with the field normal (dotted) or parallel (dash-dotted) to the GaAs layers. Lines serve as a guide to the eye.

dependence of $(dE/dt)_{ac}$ on Γ is in agreement with results of Uchimura and Uemura.[45]

Figure 11 shows the increasing energy-relaxation rate with carrier temperature for fixed B, Γ, and $n_{e,h}$. Both the increase of $(dE/dt)_{ac}$ with carrier temperature and the increase in slope of the curves with field strength B are in agreement with calculated scattering rates of Prasad and Singh.[46] To compare calculated values of $(dE/dt)_{ac}$ with the rates of carrier cooling $(dT_{e,h}/dt)$ we calculated the magnetic-field-dependent specific heat $(dE/dT_{e,h})$ for degenerate 2D carriers.[47]

In the following we use the calculated values of $dT_{e,h}/dt$ to give a quantitative explanation for the observed magnetic-field-dependent carrier cooling. To illustrate the field dependence of the cooling in 3D and 2D carrier systems more clearly, we first plot in Fig. 12 the time the carriers need to cool down to $T_{e,h} = 100$ K. For 3D carriers this time increases with B, i.e., the energy-relaxation rate reduces with increasing confinement by the magnetic field (as already discussed in Sec. IV A). Confinement of carriers in quantum-well structures at $B = 0$ T also reduces the carrier cooling with respect to 3D as was reported previously[7,8,12] for picosecond photoexcited carriers and is shown in Fig. 12 at $B = 0$ T.

For a magnetic field parallel to the 5-nm-thick GaAs layers of the quantum-well structure the carrier cooling was found to be field independent, as shown by the dashed-dotted line. This is in agreement with the fact that the cyclotron orbit diameter exceeds the quantum-well width for $B < 20$ T, which implies that wave functions and band structure of the carriers are practically not modified by the magnetic field, so that the carrier-cooling rate is unaffected.

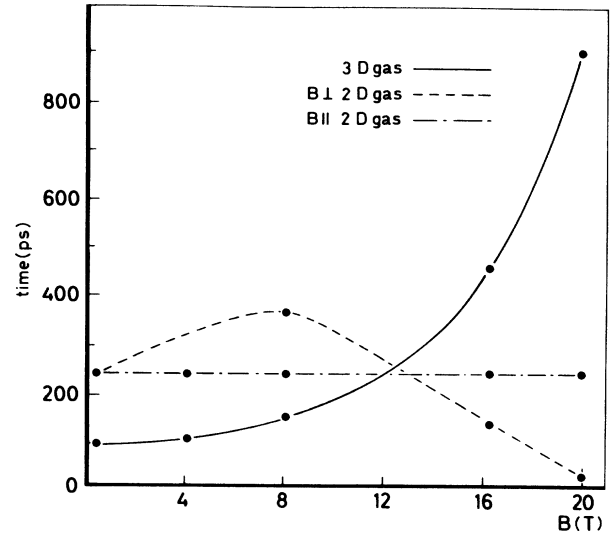However, for a magnetic field perpendicular to the 2D

GaAs layers (dashed line) the time to cool down to $T_{e,h} = 100$ K increases for $B < 8$ T (as in 3D) and subsequently decreases up to $B = 20$ T, in agreement with previous reports.[12,48] We suggest this behavior is due to decreasing relaxation rate via LO-phonon emission and an increasing relaxation rate via acoustic-phonon emission with increasing magnetic field.

In general, the energy relaxation via phonon emission is given by $dE/dt = (dE/dt)_{opt} + (dE/dt)_{ac}$. Application of a magnetic field normal to the thin GaAs layers reduces $(dE/dt)_{opt}$ as in three dimensions. However, in two dimensions the applied field completely quantizes the carrier energy to $E_{n,N} = E_n + (N + \frac{1}{2})\hbar\omega_c$ where E_n is the confinement energy. The absence of dispersion implies that the degenerate carriers (Landau-level degeneracy $eB/\hbar$) all emit LO phonons in the same wave-vector region. This further enhances the reducing effect of nonequilibrium LO phonons on the relaxation rate, and will result in a saturation of $(dE/dt)_{opt}$.[49,50] Here it must be emphasized that the density of states has a Landau-level linewidth Γ_{sc} much smaller than both the Landau-level splitting $\hbar\omega_c$ and the optical-phonon energy $\hbar\omega_{LO}$, as discussed previously. On the other hand, as shown in Fig. 10, application of a magnetic field increases $(dE/dt)_{ac}$. To sustain this quantitatively we compare the experimental and calculated cooling rates at $T_{e,h} = 100$ K for $B = 8$ and 20 T, where acoustic-phonon emission is important. From the slopes of the experimental cooling curves of Fig. 9, $dT_{e,h}/dt$ is found to vary from -0.1 K/ps at $B = 8$ T to -0.8 K/ps at $B = 20$ T, i.e., a relative enhancement by a factor of 8. Turning to the theoretical results of Figs. 10 and 11 for calculation of $(dT_{e,h}/dt)_{ac}$, one must take into account both the variation in $(dE/dt)_{ac}$ with B and Γ and the field-dependent specific heat.

From the inset of Fig. 10 it follows that for $B = 8$ T

and the experimentally determined value of $\Gamma = 10$ meV, $(dE/dt)_{ac} = 2.4 \times 10^7$ eV/s, while at $B = 20$ T and $\Gamma = 4$ meV, $(dE/dt)_{ac} = 9.5 \times 10^7$ eV/s. With use of the specific heat of the carrier gas at $T_{e,h} = 100$ K and $n_{e,h} = 1 \times 10^{18}$ cm^{-3}, which amounts to $0.5 k_B$ at $B = 8$ T and $0.39 k_B$ at $B = 20$ T,[47] $dT_{e,h}/dt$ is -0.3 K/ps and -1.8 K/ps, respectively, i.e., a relative enhancement by a factor of 6. This is in good agreement with the factor 8 experimentally obtained. The overestimation in absolute value by a factor of 3 (cf. -0.1 and -0.3 K/ps at $B = 8$ T and -0.3 and -1.8 K/ps at $B = 20$ T) may be due to the model; however, it supports the importance of acoustic-phonon emission in the energy-relaxation process. In conclusion, for $B > 8$ T energy relaxation for hot carriers in a 5-nm quantum well is well described by acoustic-phonon emission.

V. DISCUSSION

We first discuss the experimental results for bulk GaAs. For the zero-field-cooling curve (Fig. 8) a value of $C = 0.5$, i.e., $(dE/dt)_{expt} = 0.5 (dE/dt)_{theor}$ had to be used to obtain a correct fit of the data. This discrepancy between theory and experiment may be due to neglect in the model of both phonon generation during the picosecond laser pulse[18,49] and dynamical screening of the carrier-phonon interactions.[51] Inclusion of both processes is expected to give closer agreement between theory and experiment, since they reduce carrier cooling. Secondly, the description of the return to equilibrium of the optical-phonon system with a single wave-vector-independent time constant τ (Ref. 18) may be a significant simplification.

With respect to values of $C \neq 1$, in case a magnetic field is applied, the following comments can be made. (1) The model presented in Sec. IV deals with unbroadened Landau levels, and is questionable for low-field values ($B < 10$ T) where $\hbar \omega_c \approx k_B T_{e,h}$ and $\hbar \omega_c \approx \Gamma$. (2) A more exact treatment on the energy relaxation should contain the time-dependent variation of the density-of-states function (see inset of Fig. 6). (3) The behavior of dynamical screening in the presence of a magnetic field has not been studied until now. (4) The initial temperature T_0 is assumed constant for the different magnetic-field strengths.

The physics underlying the experimentally observed changes in carrier cooling GaAs can be described as follows. The photoexcited hot carriers lose their excess energy primarily by LO- and TO-phonon emission, where carrier band structure and conservation of energy and momentum determine the wave-vector range of the involved phonons. The volume occupied in carrier momentum space at $B = 0$ T is a sphere. Application of a magnetic field breaks the spherical symmetry of the carrier-momentum space, and as a consequence the relevant phonon phase-space volume, as was shown by Calecki and Lewiner for hot carriers in the extreme quantum limit.[52] It should be noted that the effect of both magnetic field and dimensionality enters only by the change of density of states. The matrix element of the electron-phonon in-

teraction is not affected.[52-54] In three dimensions, when a number of Landau levels is occupied and relaxation occurs via both intra- and inter-Landau-level transitions, the range of emitted phonon wave vectors normal to the field direction $(q_\perp)$ is determined by the Landau-level matrix elements.[39] For the direction parallel to the magnetic field (q_z) the range of emitted q_z values, allowed by the conservation laws, depends on the ratio of Landau-level splitting $\hbar \omega_c$ and optical-phonon energy E_{LO}, and is minimal[50] at the resonance conditions $N\hbar \omega_c = E_{LO}$. This implies that application of a magnetic field favors phonon emission in specific regions of $q_\perp$ and q_z, which leads to large phonon populations of particular modes. The prediction by Pormotsev,[49] that this narrowing in wave-vector ranges results in decreased energy-relaxation rate, and a suppression of the magnetophonon resonances is in agreement with results for 3D carriers in Figs. 8 and 10.

Application of a strong magnetic field normal to the 2D carrier gas leads to quasi-zero-dimensional carrier states. The absence of dispersion, and the fact that intra-Landau-level scattering is not allowed (the optical-phonon energy, $\hbar \omega_{LO} = 36$ meV, exceeds the Landau-level linewidth, $\Gamma_{sc} < 7$ meV, at all field strengths) leads to a further suppression of the relaxation via optical-phonon emission. These two effects, together with the effect that in a 5-nm well only one electronic subband is present, imply that for $B > 8$ T energy relaxation by optical-phonon emission has reduced so much that acoustic-phonon emission takes over.

The magnetic-field value at which the carrier cooling is minimal depends, via the scattering rates, on excitation conditions and well width. As follows from the experimental results, for a quantum-well width of 5 nm and an excited carrier density of $n_{e,h} = 3 \times 10^{18}$ cm^{-3} the transition to enhancement in cooling rate is observed around $B = 8$ T.

The fact that the cooling rate slows down in bulk GaAs indicates that even in the presence of nonequilibrium LO phonons the contribution to the energy relaxation by acoustic-phonon emission is still relatively small up to $B = 20$ T. An enhancement of the carrier cooling as observed in two dimensions above $B = 8$ T is expected to occur at field values above $B = 20$ T, since the magnetic-field dependence of the carrier-acoustic-phonon interaction is likely to be similar in both carrier systems.

As observed for both 3D and 2D carriers (Figs. 8 and 9) the carrier temperature does not fall below 40 K within the carrier lifetime. Lattice heating should follow as a result of energy transfer from optical phonons to acoustic phonons or via direct carrier-acoustic-phonon coupling. However, since the acoustic-phonon phase space is large, its deviation from equilibrium is expected to be negligible. Besides, an increase in lattice temperatures has no effect on the magnetic-field dependence of the carrier-phonon interaction rates. In conclusion, we have shown that (1) the energy-relaxtion rate of photoexcited hot carriers in bulk GaAs reduces with increasing magnetic-field strength. This effect is well described by a model containing the magnetic-field-dependent kinetics of the carrier-nonequilibrium-LO-phonon system. (2) For the quantum-well structure, application of a magnetic field

parallel to the GaAs layers leaves the cooling rate unaffected, as long as the cyclotron orbit diameter exceeds the quantum-well width. For a field normal to the layers, carrier cooling initially reduces up to $B = 8$ T and speeds up at higher-field values up to $B = 20$ T. This behavior is suggested to be due to a reduced relaxation by optical-phonon emission (as in three dimensions) and an increasing relaxation via acoustic-phonon emission.

*Present address: Philips Research Laboratories, NL-5600 JA Eindhoven, The Netherlands.

†Also at Hochfeld-Magnetlabor, Max-Planck-Institut für Festkörperforschung, Boîte Postale 166X, F-38042 Grenoble Cédex, France.

[1]L. Esaki, IEEE J. Quantum Electron. QE-22, 1611 (1986).

[2]P. M. Petroff, A. C. Gossard, R. A. Logan, and W. Wiegmann, Appl. Phys. Lett. 41, 635 (1982).

[3]Y. Arakawa and A. Yariv, IEEE J. Quantum Electron. QE-22, 1887 (1986).

[4]P. J. Price, Physica (Utrecht) 134B+C, 164 (1985).

[5]H. Sakaki, Y. Arakawa, M. Nishioka, J. Yoshino, H. Okamoto, and N. Miura, Appl. Phys. Lett. 46, 83 (1985).

[6]C. V. Shank, R. L. Fork, R. Yen, J. Shah, B. I. Greene, A. C. Gossard, and W. Wiegmann, Solid State Commun. 47, 981 (1983).

[7]J. F. Ryan, R. A. Taylor, A. J. Tuberfield, A. Maciel, J. Worlock, A. C. Gossard, and W. Wiegmann, Phys. Rev. Lett. 53, 1841 (1984).

[8]Z. Y. Xu and C. L. Tang, Appl. Phys. Lett. 44, 692 (1984).

[9]K. Kash, J. Shah, D. Block, A. C. Gossard, and W. Wiegmann, Physica (Utrecht) 134 B+C, 189 (1985).

[10]J. Shah, A. Pinczuck, A. C. Gossard, and W. Wiegmann, Phys. Rev. Lett. 54, 2045 (1985).

[11]R. W. J. Hollering, T. T. J. M. Berendschot, H. J. A. Bluyssen, P. Wyder, M. Leys, and J. Wolter, Physica (Utrecht) 134B+C, 422 (1985).

[12]R. W. J. Hollering, T. T. J. M. Berendschot, H. J. A. Bluyssen, P. Wyder, M. Leys, and J. Wolter, Solid State Commun. 57, 527 (1986).

[13]C. V. Shank, R. L. Fork, R. F. Leheny, and J. Shah, Phys. Rev. Lett. 42, 112 (1978).

[14]D. von der Linde and R. Lambrich, Phys. Rev. Lett. 42, 1090 (1979).

[15]S. Tanaka, H. Kobayashi, and S. Shionoya, J. Phys. Soc. Jpn. 49, 1051 (1981).

[16]W. Graudzus and E. O. Göbel, Physica (Utrecht) B117+118, 555 (1981).

[17]J. Shah, J. Phys. (Paris) Colloq. 42, C 7-445 (1981).

[18]W. Pötz and P. Kocevar, Phys. Rev. B 28, 7040 (1983).

[19]W. W. Rühle and H. J. Polland, Phys. Rev. B 36, 1683 (1987).

[20]M. R. Leys, C. van Opdorp, M. P. A. Viegers, and H. J. A. Talen van der Mheen, J. Cryst. Growth 68, 431 (1984).

[21]H. Mahr and M. D. Hirsch, Opt. Commun. 13, 96 (1974).

[22]K. Kash and J. Shah, Appl. Phys. Lett. 45, 401 (1984).

[23]J. Shah, Solid State Electron. 21, 43 (1978).

[24]C. Weisbuch, R. Dingle, A. C. Gossard, and W. Weigmann, Solid State Commun. 30, 709 (1981).

[25]K. Shum, P. P. Ho, R. R. Alfano, D. F. Welch, G. W. Wichs, and L. F. Eastman, IEEE J. Quantum Electron. QE-22, 1811 (1986).

[26]R. Dingle, Proc. R. Soc. London, Ser. A 211, 517 (1962).

[27]L. M. Roth and P. N. Argyres, in Semiconductors and Semimetals (Academic, London, 1966), Vol. 1.

[28]R. C. G. M. Smetsers, A. F. van Ettger, and H. J. A. Bluyssen, Semicond. Sci. Technol. 1, 121 (1986).

[29]R. Kubo, N. Hashitsume, and S. J. Myake, in Solid State Physics, edited by H. Ehrenreich, F. Seitz, and D. Turnbull (Academic, London, 1966), Vol. 17, p. 269.

[30]S. Chaudjuri and K. K. Bajaj, Phys. Rev. B 29, 7085 (1984).

[31]R. Ulbrich, Phys. Rev. B 6, 5719 (1973).

[32]T. Ando, A. Fowler, and F. Stern, Rev. Mod. Phys. 54, 427 (1982).

[33]R. C. Miller, D. A. Kleinmann, and A. C. Gossard, Phys. Rev. B 29, 7085 (1984).

[34]M. Altarelli, U. Ekenberg, and A. Fasolino, Phys. Rev. B 32, 5138 (1985).

[35]S. R. E. Yang and L. J. Sham, Phys. Rev. Lett. 24, 2598 (1987).

[36]H. Haug and D. B. Tran Thoai, Phys. Status Solidi B 98, 581 (1980).

[37]J. Shah, IEEE J. Quantum Electron. QE-22, 1728 (1986).

[38]R. W. J. Hollering, T. T. J. M. Berendschot, H. J. A. Bluyssen, H. A. J. M. Reinen, and P. Wyder, in The Application of High Magnetic Fields in Semiconductor Physics, Vol. 71 of Springer Series in Solid State Physics, edited by G. Landwehr (Springer, Berlin, 1986), p. 466.

[39]G. Bauer, H. Kahlert, and P. Kocevar, Phys. Rev. B 11, 968 (1975).

[40]K. Hess, T. Englert, T. Neugebauer, G. Landwehr, and G. Dorda, Phys. Rev. B 16, 3652 (1977).

[41]E. M. Conwell, High Field Transport in Semiconductors (Academic, New York, 1967).

[42]P. J. Price, Ann. Phys. (N.Y.) 133, 217 (1981).

[43]H. A. J. M. Reinen, T. T. J. M. Berendschot, R. J. H. Kappert, and H. J. A. Bluyssen, Solid State Commun. 65, 1495 (1988).

[44]T. T. J. M. Berendschot, H. A. J. M. Reinen, and H. J. A. Bluyssen, Solid State Commun. 63, 873 (1987).

[45]Y. Uchimura and Y. Uemura, J. Phys. Soc. Jpn. 47, 1417 (1979).

[46]M. Prasad and M. Singh, Phys. Rev. B 29, 2324 (1984).

[47]T. T. J. M. Berendschot, thesis, University of Nijmegen, 1985.

[48]J. F. Ryan, R. A. Taylor, A. J. Tuberfield, and J. M. Worlock, Proc. Yamada Conf. XIII, 712 (1985).

[49]R. V. Pormotsev and G. I. Kharus, Fiz. Tverd. Tela (Leningrad) 9, 2870 (1967) [Sov. Phys.—Solid State 9, 2256 (1968)].

[50]R. Luzzi, in *Semiconductors Probed by Ultrafast Laser Spectroscopy*, edited by R. Alfano (Academic, New York, 1984), Vol. 1.

[51]C. A. Yang and S. A. Lyon, Physica (Utrecht) **134B+C**, 309 (1985).

[52]C. Calecki and D. Lewiner, Solid State Electron. **21**, 185 (1978).

[53]P. J. Price, Superlatt. Microstruct. **1**, 255 (1985).

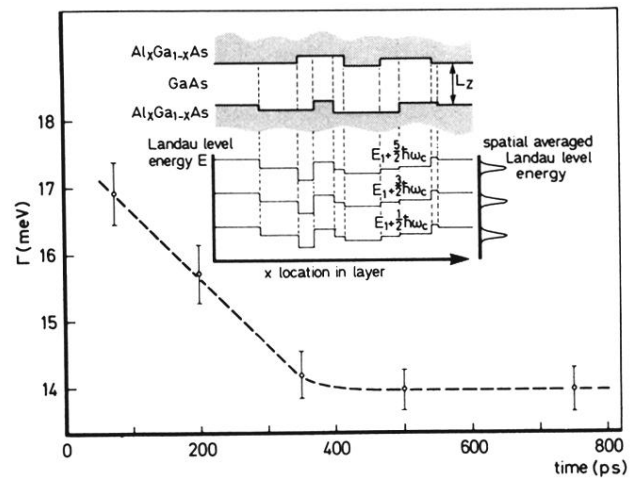[54]D. Bimberg, D. Mars, J. N. Miller, R. Bauer, D. Oertal, and J. Christen, Superlatt. Microstruct. **3**, 79 (1987).

FIG. 7. Evolution of the Landau-level linewidth $\Gamma(t)$ in a GaAs/Al$_{0.6}$Ga$_{0.4}$As quantum-well structure for $B = 20$ T, as obtained by fitting the spectra of Fig. 4. The line is drawn as a guide to the eye. The inset shows the contribution to the Landau-level broadening as a result of spatial averaging over the varying Landau-level energies caused by well-width fluctuations.